

Simultaneous prestack seismic inversion in a carbonate reservoir

<http://dx.doi.org/10.1590/0370-44672016710024>

Rafael Amaral Cataldo

Mestre

Universidade Estadual de Campinas – UNICAMP

Instituto de Geociências

Campinas - São Paulo – Brasil

rac.cataldo@gmail.com

Emilson Pereira Leite

Professor-Doutor II

Universidade Estadual de Campinas – UNICAMP

Instituto de Geociências

Campinas - São Paulo – Brasil

emilson@ige.unicamp.br

Abstract

We applied a method of Simultaneous Prestack Seismic Inversion (SPSI) in a hydrocarbon field located in the Campos Basin, Brazil. The goal was to study the application of this method to Albian carbonate rocks of the Quissamã Formation. Based on what is found in nearby fields, this Formation potentially contains hydrocarbon accumulations that can be revealed with the inverted models. P-wave velocity (V_p), S-wave velocity (V_s) and density (ρ) curves along seven wells were used as inputs to construct 3-D initial models of acoustic impedance (Z_p), shear impedance (Z_s) and ρ . Wells without V_s and ρ curves had those values calculated from well-established equations. Final 3-D models were calculated from deviations in linear relationships between the logarithms of Z_s and Z_p , as well as between ρ and Z_p , which were merged with the initial models. Interpretations of the inversion results were conducted based on patterns found along well logs such as resistivity (ILD), gamma ray (GR), density (RHOB), neutron porosity (NPHI) and sonic (DT). These analyses provided criteria to select the best inverted models. These models show low impedance anomalies that are consistent with previous studies performed with the well logs. One well in particular was interpreted as having high potential to contain hydrocarbons. This well shows an impedance pattern that allowed us to highlight other areas with the same pattern throughout the entire seismic volume.

Keywords: prestack seismic inversion; carbonate reservoir; Campos basin.

1. Introduction

In the last few decades the oil industry has been focusing on the improvement of various methods to solve current geological problems, such as the modeling of pre-salt carbonate reservoirs in Brazil. Poststack, prestack and elastic seismic inversions are among those methods that assist the characterization of hydrocarbon reservoirs. Latimer *et al.* (2000) points out that it is common to find empirical relationships between Z_p and rock properties such as lithology and porosity. Even though the Z_p model can provide such information, it does not discriminate porosities between carbonates and shales (Li *et al.*, 2003). However, when we analyze Z_p , Z_s and ρ models together, we can reinforce this hypothesis because the extraction of multiple elastic properties from seismic data enhances the probability of identifying different rock groups (see e.g. Jarvis *et al.*, 2007).

The prestack inversion emerges from

the need for extracting more information from seismic data to solve geological problems that are not answered by poststack inversion. The V_s information used in prestack seismic inversion can solve, e.g. the duality between porosity in carbonates and shales, in which Z_p alone cannot solve. Therefore, the S-wave information is crucial to discriminate among reservoir and non-reservoir rocks (Li *et al.*, 2003). In this context, SPSI is considered to be the ultimate method that combines AVO data with seismic inversion techniques (Goffey, 2013).

One of the obstacles in applying SPSI to carbonate rocks is that, in contrast with sandstones, these lithotypes are vertically and laterally heterogeneous and represent a complex challenge regarding reservoir characterization. Being mainly of biological origin, carbonates have complex textures and are susceptible to diagenesis modifications, leading to mineralogy and

pore structure changes that make these rocks more difficult to model (Eberli *et al.*, 2003).

Over the past few years several studies were performed in different lithologies proving the effectiveness of prestack seismic inversion methods. For example, poststack analysis on argillaceous carbonates and breccias may not differentiate reservoir from non-reservoir rocks (dolomitic and calcitic shales), but SPSI combined with V_p/V_s analysis may enable the separation of these lithotypes (Liu *et al.*, 2012). Benabentos *et al.* (2007) applied prestack inversion to assist the selection of well locations to drill in Burgos Basin, Mexico, where the targets were sandstones potentially containing gas accumulations. AlMuhaidib *et al.* (2012) used impedance volumes generated from SPSI to estimate porosity values on a Jurassic Saudi Arabia carbonate field. The results pointed out to new potential hydrocarbon areas of good quality.

The main goal of this paper is to study the advantages and limitations of recovering petrophysical parameters from a carbonate reservoir using SPSI (Hampson *et al.*, 2006). We have conducted a sensitivity analysis on parameters required to invert prestack data with this method. We

Geological setting

Campos Basin has the second most productive hydrocarbon reservoirs in Brazil, encompassing ~50% of oil and ~22% of natural gas production (ANP, 2017). The A field is located in southeast of Campos Basin, Brazil, covering an area of 32 km² in water depths of ~100 m. Considering our zone of interest at the Quissamã Formation, it is composed of oolitic/oncolithic and peloidal calcarenites, calcirudites and calcilutites. In terms of trapping, this reservoir is essentially structural-stratigraphic where

Data and software

The inversions were carried out using the software HRS-9 (CGG-Veritas). The seismic data consists of partially stacked Common Mid Point (CMP) gathers recorded into four angle stack files: 4° to 13°; 13° to 22°; 22° to 31°; and 31° to 40°. The seismic data were previ-

ously processed so that no additional deconvolution or filtering was required before the application of SPSI. V_p , V_s and ρ were obtained from well logs. These data are needed to build the initial models for all prestack inversions. The area covered by prestack data includes a total

of seven wells containing the following logs: RHOB, GR, ILD, NPHI and DT. Two horizons were extracted based on seismic reflections representing the top of Quissamã Formation and Lagoa Feia. Table 1 summarizes the main information about the data.

obtained 3-D models of Z_p , Z_s and ρ of a post-salt carbonate reservoir of Macae Group, located in Campos Basin, offshore Brazil. We refer to this oil field as the “A” field. The A field contains albian carbonate rocks of Quissamã Formation that were deposited in a shallow platform environment.

These rocks have a porosity of ~25% and permeability of ~250md (Spadini, 1992). This reservoir is responsible for 31% of in-place oil volume of the A field, but has a recovery factor of ~15.40% (Horschutz *et al.*, 1992). This is the first application of SPSI for this oil field.

oolithic/oncolithic calcarenite banks with a thickness of up to 15 m. These reservoirs generally show high porosities associated to variable values of permeability. The reservoirs are composed of carbonate sand banks elongated to northeast, which in turn are composed mainly of grainstones and packstones. The porosity of these carbonates is essentially intergranular and has unexpressive secondary porosity formed by dissolution of oncoliths nuclei and vugular porosity (Spadini & Paumer, 1983).

Seismic acquisition sample rate	4 ms
Seismic trace length	2500 ms
Number of samples per seismic trace	625
Number of inlines & xlines	404 & 479
Distance between inlines & xlines	12.50 m
Wells	A1, A2, A3, A4, A78, A153 and A156
Horizons	Quissamã and Lagoa Feia

Table 1
Main information about seismic data acquisition parameters and well logs.

2. Methods

Seismic inversion requires four main steps: (i) create an initial impedance model of low frequencies from elastic properties; (ii) extract wavelet(s) from seismic-well ties; (iii) do a relative inversion and; (iv) merge the relative inversion results with the initial models. Firstly, an “inversion analysis” is carried out by applying step (iv) only along the wells. Then, the SPSI is applied to the complete seismic volume using the optimal parameters selected from the inversion analysis.

Firstly we calculated V_s logs using two formulas. The first is that of Castagna *et al.* (1985) and was used for the external part of Quissamã Formation. For

the internal part of Quissamã Formation we used the formula shown in Greenberg & Castagna (1992). Pinheiro (2005) obtained high positive correlations between this formula and experimental results in coquina samples from Lagoa Feia Formation located in Campos Basin. Wells A1, A4 and A153 did not contain the RHOB logs within the reservoir interval and these values were calculated by the Gardner’s equation (Gardner *et al.*, 1974).

To create the initial low-frequency models, we used the Quissamã and Lagoa Feia top horizons as stratigraphic surfaces. Seismic-well ties were conducted with all wells in order to adjust seismic events to

well log markers and to make depth-time conversions. To accomplish this step, we extracted and tested wavelets based on Walden and White (1998) and White & Simm (2003). In our case, the best wavelet has a wavelength of 60 ms and a frequency peak of ~25 Hz. For each well, a Z_p log was generated from RHOB and DT in order to obtain reflectivity values. The convolution of a reflectivity series with a wavelet provides a synthetic seismogram which is compared with the original seismogram. Having converted wells from depth to time and positioned them correctly within the seismic data volume, the initial Z_p , Z_s and ρ models were created.

Simultaneous prestack seismic inversion (SPSI)

The SPSI method assumes that the seismic trace can be modeled by the well-known 1-D convolutional model. For small values, the reflectivity (\mathbf{R}_p) calculated by a recursive equation using Z_p can be approximated by (Russell and Hampson, 1991)

$$\mathbf{R}_{p_i} \approx 1/2 \Delta \ln(\mathbf{Z}_{p_i}) = 1/2 [\ln(\mathbf{Z}_{p_{i+1}}) - \ln(\mathbf{Z}_{p_i})] \quad (1)$$

where i is the i^{th} interface between layers i and $i+1$. For all layers, equation 1 can be written in matrix form as

$$\begin{bmatrix} R_{p1} \\ R_{p2} \\ \vdots \\ R_{pN} \end{bmatrix} = \frac{1}{2} \begin{bmatrix} -1 & 1 & 0 & \dots \\ 0 & -1 & 1 & \ddots \\ 0 & 0 & -1 & \ddots \\ \vdots & \ddots & \ddots & \ddots \end{bmatrix} \begin{bmatrix} L_{p1} \\ L_{p2} \\ \vdots \\ L_{pI} \end{bmatrix} \quad (2)$$

where $L_{p_i} = \ln(Z_{p_i})$, and the matrix with zeros and ones is denoted by \mathbf{D} . By representing the seismic trace (\mathbf{T}) as a convolution between a seismic wavelet (\mathbf{w}) and \mathbf{R}_p , we obtain

$$\begin{bmatrix} T_1 \\ T_2 \\ \vdots \\ T_N \end{bmatrix} = \frac{1}{2} \begin{bmatrix} W_1 & 0 & 0 & \dots \\ W_2 & W_1 & 1 & \ddots \\ W_3 & W_2 & W_1 & \ddots \\ \vdots & \ddots & \ddots & \ddots \end{bmatrix} \begin{bmatrix} L_{p1} \\ L_{p2} \\ \vdots \\ L_{pI} \end{bmatrix} \quad (3)$$

where T_i is the i^{th} sample of the seismic trace, w_j is the j^{th} term of \mathbf{w} and the wavelet matrix is denoted by \mathbf{W} . By combining equations (2) and (3) we have (Russell and

Hampson, 1991):

$$\mathbf{T} = (1/2) \mathbf{WDL}_p \quad (4)$$

Equation 4 represents a zero-offset seismic trace. For prestack data with different incident angles (θ), a modified version of the Aki-Richards approximations is used (Fatti *et al.*, 1994), leading to an analogous equation for the prestack trace

$\mathbf{T}(\theta)$. Also, the SPSI assumes a linear relationship among the logarithms L_p ($\ln Z_p$), L_s ($\ln Z_s$) e L_d ($\ln \rho$) (Russell *et al.*, 2006):

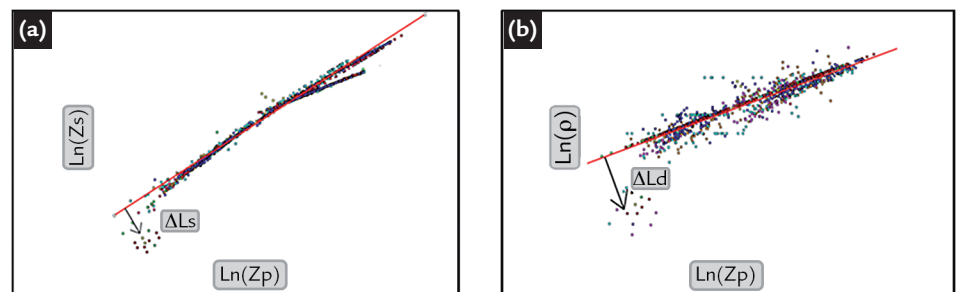
$$L_s = k L_p + k_c + \Delta L_s \quad (5)$$

$$L_d = m L_p + m_c + \Delta L_d \quad (6)$$

Therefore, the essence of the method is to calculate ΔL_s and ΔL_d from linear models fitted to the background values using Z_p , Z_s and ρ (Figure 1). Parameters k , k_c , m and m_c

are fitted coefficients. These deviations may reflect areas where hydrocarbons are present.

Figure 1
(a) $\ln(Z_s)$ vs. $\ln(Z_p)$.
(b) $\ln(\rho)$ vs. $\ln(Z_p)$. Red lines are background linear models. The deviations from these models, ΔL_s and ΔL_d , are hydrocarbon anomalies (Russell *et al.*, 2006).



By combining equations (4) to (6) into $\mathbf{T}(\theta)$, we obtain

$$\mathbf{T}(\theta) = \hat{c}_1 \mathbf{W}(\theta) \mathbf{DL}_p + \hat{c}_2 \mathbf{W}(\theta) \mathbf{DL}_s + \mathbf{W}(\theta) c_3 \mathbf{DL}_d \quad (7)$$

where $\hat{c}_1 = (1/2)c_1 + (1/2)k_{c2} + m_{c3}$, $\hat{c}_2 = (1/2)c_2$, $c_1 = 1 + \tan^2 \theta$, $c_2 = -8\gamma \tan^2 \theta$ and $c_3 = -0.5 \tan^2 \theta - 2\gamma \sin^2 \theta$, $\gamma = V_s/V_p$. Equation 7 is a system of linear equations to which

the solution is a vector $\mathbf{p} = [L_p \Delta L_s \Delta L_d]$ (Russell *et al.*, 2006).

3. Results and discussion

Seismic-well ties provided correlations from 0.622 to 0.739 between synthetic and observed seismic traces.

Two horizons representing the Quissamã and Lagoa Feia top formations were interpreted by picking seismic amplitude

events in all inlines and xlines available. As an example, we present the results near well A153 because they show the highest

probability of having oil.

It was not possible to directly attach different values of Z_p , Z_s and ρ to the lithotypes of this field, because there were not available cores along the wells to constrain such kind of interpretation. Thus, all interpretations were conducted only with the log readings from the seven wells.

The reader may ask if the output frequencies are being generated only from the initial model, so that the final results have

only log frequencies without information from seismic data. As Figure 2 shows, the initial model is significantly different from the final model denoting that seismic frequencies have a critical impact on the final results.

The “inversion analysis” allowed us to visually and numerically compare the inversion results along the wells before applying the inversion process to all available seismic traces (Figure 3). Correlations

between $\ln(Z_p)$, $\ln(Z_s)$ and ρ , calculated or extracted from the wells, and those generated by the inversion were analyzed. At the same time, correlations between synthetic and real seismic traces were monitored. Figure 3 shows the inversion result for well A153, and although it does not recover all events, it follows the trend of the derived logs and initial models. This is explained by the difference between seismic and log resolution.

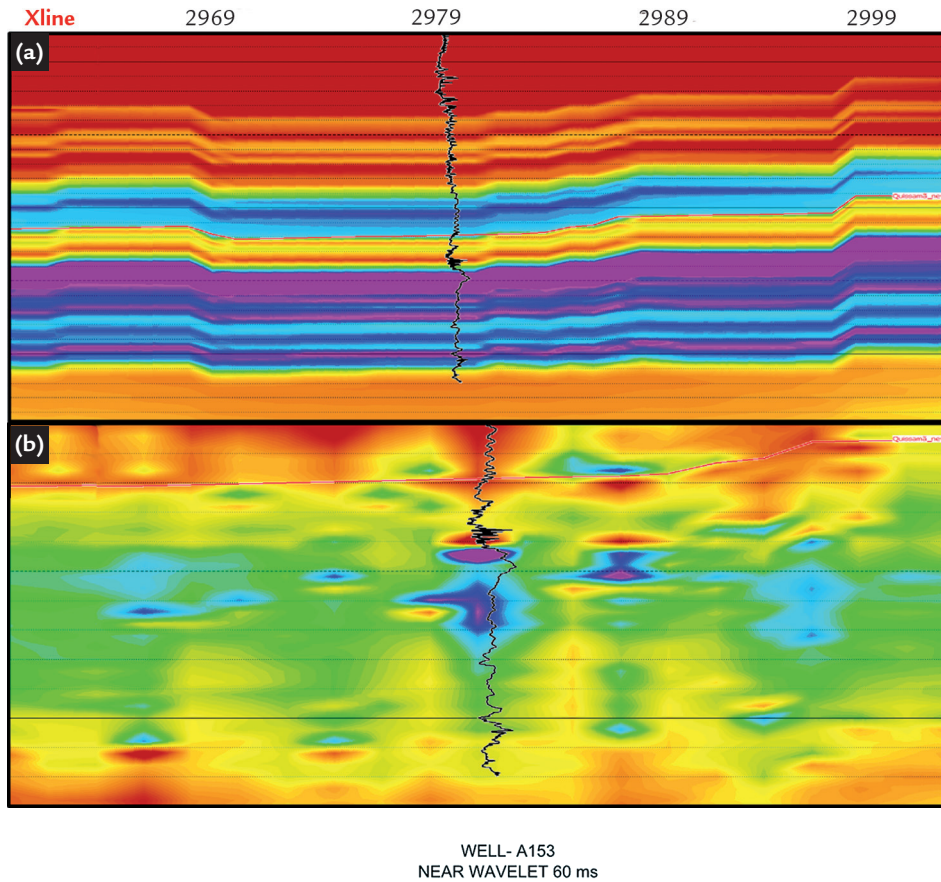


Figure 2 Comparison between initial (a) and final model (b) for near well A153 at inline 2171.

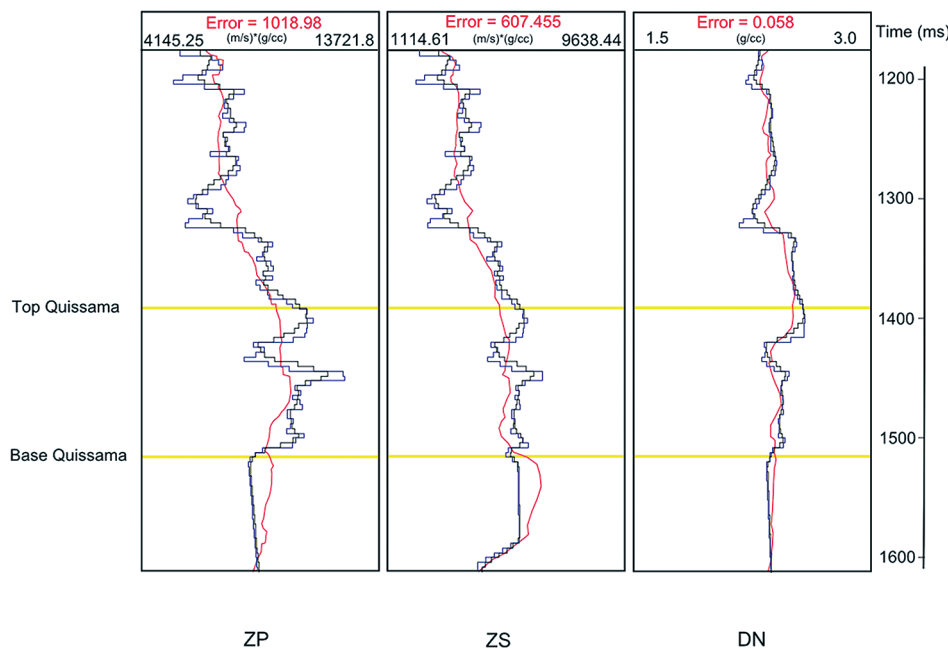


Figure 3 Example of the “inversion analysis” results along well A153. Yellow lines represent top and base of the Quissamã Formation. Blue curves represent derived P-wave (Z_p) and S-wave (Z_s) impedance and density (ρ) values. Red and black curves represent initial and final inversion model, respectively.

The final step was to perform the SPSI for all seismic traces using parameters that point to a higher reliability of the process. It is important to notice that several wavelets with distinct features, as well as different filters and pre-whitening values were tested before running the final inversion. Empirically, we have noticed that an initial low frequency model without filter presents better results, meaning this was the only model that results in an anomaly exactly where the well A153 presents favorable indicators of oil presence (Rider, 2004). The influence of the wavelet on the error and correlation is low, but the level of the pre-whitening applied results in significant differences, especially if we look at well A153 for both correlation and error values. This was a key factor to get better results on the final volumes. The wavelet was extracted statistically from the seismic data partially stacked from 4° to 13°. We also

used a pre-whitening of 5% to stabilize the inversion process.

In general, the Z_p , Z_s and ρ models are consistent with each other. We decided not to plot the well log curves on the models because they would cover some interesting anomalies that were found on well locations. Well logs present on well A153 show favorable results for hydrocarbon presence between 1420 to 1435 ms. Within this interval, this well shows an ILD and NPHI trend increasing downward, while V_p , V_s , GR, SP and RHOB curves show a decreasing pattern when compared to readings above this interval. The increase on ILD and NPHI logs, together with a decrease on GR and SP (except between 1426 - 1428 ms), may indicate the presence of hydrocarbons. In other words, this interval indicates an area with higher porosity and permeability when compared to surrounding areas, besides the presence of a fluid with greater ILD values

and less amount of clays. It is important to notice that the increase in NPHI is not associated to an increase in clay content because the GR log is decreasing, so we may predict that we are dealing with a higher porosity interval. As V_p , V_s and RHOB values also decrease, we expected a low impedance anomaly in the same interval for this well.

To better visualize it, low impedance anomalies are displayed with arrows that points to these features in Figure 4. We may observe in the Z_p model of Figure 4A that the xline 2979, where well A153 is located, shows low impedance values (~9200 (m/s)*(g/cc)) around 1430-1440 ms. As we can see in the Z_s and ρ models, the same anomaly is recognized in the same interval, depicted by green and yellow colors, respectively. In the ρ model (Figure 4c) there is a smooth ellipse that is recognizable, but all three models are compatible with the analysis conducted for the well logs.

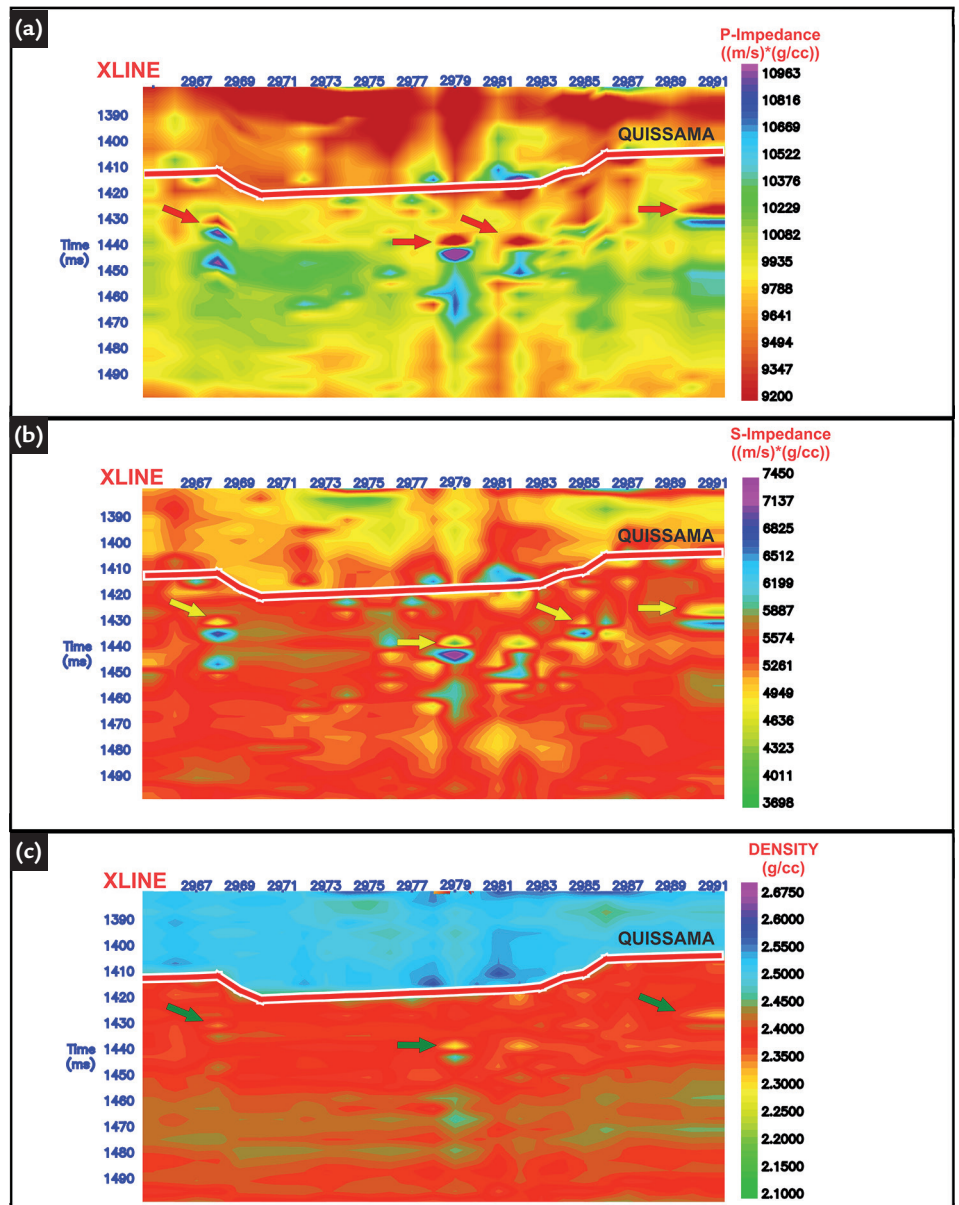


Figure 4
Final models of Z_p (A), Z_s (B) and ρ (C) near well A153 extracted along inline 2171.

It is possible to extend these predictions from xlines 2967 to 2969, 2981 to 2983 and 2989 to 2991 because they occur in the same interval where we have found the low impedance anomaly along well A153. The reader should notice the pattern of these anomalies at distances approximately constant from the Quissamã horizon, which may be associated to reservoirs found in other fields of the Campos Basin (see arrows in Figure 4). We also looked for the same anomalies in the same interval throughout the final inversion volumes. This search was carried out for all inverted volumes and we found

4. Conclusions

In general, the inverted models present high correlations with the actual logs and may indicate areas with a high probability of finding hydrocarbon accumulations. This conclusion is based on the assumption that the Quissamã Formation contains hydrocarbon reservoirs and thus, we looked for low impedance anomalies followed downward by high anomalies which are consistent

significant anomalies from inline 2170 to 2173 and from xlines 2989 to 2994.

Another way to check the inversion quality is by cross-plotting the inverted models versus the actual logs. From such cross-plots, we noticed that the errors in the ρ model are the lowest while the errors in the Z_s model are the highest. However, the ρ model should be interpreted with caution, because the prestack data used in this work does not have incident angles higher than 40° . In most cases, this is not enough to solve ρ models with reliability. Seismic data has a low signal/noise when registered at

with well log interpretation.

The lowest inversion errors were obtained for the ρ model while the Z_s model shows the highest errors. However, there is absence of incident angles above 40° . This model should be interpreted together with the other models, in order to check for consistency and to get a better understanding of the distribution of anomalies.

high angles. Shi *et al.* (2010) points out that the near offset seismic amplitudes are mainly controlled by velocity, and that only the far offset amplitudes may record ρ information.

We could not compare our inverted models with the geology of the A field more directly, because there were no core samples and petrophysical data available. Particularly, the lack of petrophysical data led to the use of data from analog rocks to estimate, for instance, the velocity of S-wave. Certainly, the acquisition of S-wave and density logs along all wells should improve the SPSI results.

Based on the favorable results obtained in this work with well A153, we may conclude that the SPSI method applied in this work has the potential of finding anomalies related to hydrocarbon reserves in carbonate rocks of the A field. However, it must be emphasized that, to achieve optimum results, stratigraphic control, petrophysical and core data should be used as constraints.

References

- ALMUHAIDIB, A.M., SEN, M.K., TOKSOZ, M.N. Integration of geology, rock physics, logs, and prestack seismic data for reservoir porosity estimation. *AAPG Bulletin*, v. 96, n. 7, p. 1235-1251, 2012.
- ANP. Boletim da Produção de Petróleo e Gás Natural. Agência Nacional do Petróleo, Gás Natural e Biocombustíveis, Superintendência de Desenvolvimento e Produção – SDP. Ed. n. 85, set. 2017. 33p. Disponível em: <www.anp.gov.br>. Acesso em: 6 nov. 2017.
- BENABENTOS, M., SILVA, M., ORTIGOSA, F., MERCADO, V. Reservoir characterization in Burgos Basin using simultaneous inversion. *The Leading Edge*, v. 26, n. 5, p. 556-561, 2007.
- EBERLI G.P., BAECHELE, G.T., ANSELMETTI, F.S., INCZE, M.L. Factors controlling elastic properties in carbonate sediments and rocks. *The Leading Edge*, n. 22, p. 654–660, 2003.
- FATTI, J.L., SMITH, G.C., VAIL, P.J., STRAUSS, P.J., LEVITT, P.R. Detection of gas in sandstone reservoirs using AVO analysis: a 3-D Seismic Case History Using the Geostack Technique. *Geophysics*, n. 59, p. 1362-1376, 1994.
- GOFFEY, R. *AVO, inversion or AVO inversion? Hampson-Russel's software solution*. GDS Publishing Ltd., 2013.
- GARDNER, G.H.F., GARDNER, L.W., GREGORY, A.R. Formation velocity and density - the diagnostic basics for stratigraphic traps. *Geophysics*, v. 39, n. 6, p. 770-780, 1974.
- GREENBERG, M.L., CASTAGNA, J.P. Shear-wave velocity estimation in porous rock: theoretical formulation, preliminary verification and applications. *Geophysical Prospecting*, n. 40, p. 195-209, 1992.
- HAMPSON, D., RUSSELL, B.H., BANKHEAD, B. 2006. Simultaneous inversion of pre-stack seismic data. *Geohorizons*, v. 11, n. 1, p. 13-17, 2006.
- HORSCHUTZ, P. M. C., FREITAS, L. C. S., STANK, C. V., BARROSO, A. S., CRUZ, W. M. The Linguado, Carapeba, Vermelho and Marimbá Giant Oil Fields, Campos Basin, Offshore Brazil. In: HALBOUTY, M. T. (Ed.). *Giant Oil and Gas Fields of the Decade 1978-1988: AAPG Memoir 54*, p. 137–156, 1992.

- JARVIS, K., FOLKERS, A., SAUSSUS, D. Reservoir compartment prediction of the Simpson field from the geostatistical inversion of AVO seismic data. *ASEG*, p. 1-3, 2007.
- LATIMER, R. B., DAVISON, R., VAN RIEL, P. An interpreter's guide to understanding and working with seismic-derived acoustic impedance data. *The Leading Edge*, n. 19, p. 242-256, 2000.
- LI, Y., DOWNTON, J., GOODWAY, B. Recent applications of AVO to carbonate reservoirs in the Western Canadian Sedimentary Basin. *The Leading Edge*, v. 22, n. 7, p. 670-674, 2003.
- LIU, Z., SUN, S. Z., WANG, H., LU, H., ZHANG, J. Complex lithological reservoir prediction through pre-stack simultaneous inversion: a case study from the Leijia Area in Liaohe Oil-field, China. *SEG Technical Program Expanded Abstracts*, p. 1-6, 2012.
- PINHEIRO, J. E. F. Aprendendo a confiar em Greenberg-Castagna. In: INTERNATIONAL CONGRESS OF THE BRAZILIAN GEOPHYSICAL SOCIETY, 9. Brazil: 2005.
- RIDER, M. *The geological interpretation of well logs*. (2nd. Ed.). Whittles Publishing Services, 2004. p. 280.
- ROBAINA, L. E. S., FORMOSO, M. L. L., SPADINI, A. R. Carbonatos reservatório da Formação Macaé, bacia de Campos, RJ, Brasil (parte 1) – Contribuição à geoquímica dos carbonatos. *Geochim. Brasil*, v. 5, n. 1/2, p. 53-67, 1991.
- RUSSELL, B. H., HAMPSON, D. P. A comparison of post-stack seismic inversion methods. In: *Ann. Mtg. Abstracts, Society of Exploration Geophysicists*, p. 876-878, 1991.
- RUSSELL, B. H., HAMPSON, D. P., BANKHEAD, B. Simultaneous inversion of pre-stack seismic data. In: INT. CONFERENCE & EXPOSITION OF PETROLEUM GEOPHYSICS, 6. p. 371-376, 2006.
- SHI, Y. M., YAO, F. C., SUN, H. S., QI, Li. *Density inversion and porosity using seismic data*. Beijing, China: Research Institute of Exploration and Development, PetroChina, 2010.
- SPADINI, A. R. *Processo deposicionais e ciclicidade em carbonatos albianos de plataforma rasa da bacia de Campos*. Rio de Janeiro: Univ. Fed. do Rio de Janeiro, Instituto de Geociências, 1992. 139 p. (Dissertação de Mestrado).
- SPADINI, A. R., PAUMER, L. M. *Os reservatórios Macaé no Campo de Pampo: o meio poroso e sua relação com as fácies deposicionais e a diagênese*. Petrobrás/Cenpes: 1983. 53p. (Relatório Interno).
- WHITE, R. E., SIMM, R. Tutorial: good practice in well ties. *First Break*, v. 21, Issue 10, p. 75-83, 2003.

Received 19 February 2016-Accepted 3 November 2017.